The Experimental and Theoretical Effect of Fire on the Structural Behavior of Laced Reinforced Concrete Deep Beams

Abbas Kareem
Civil Engineering Department, College of Engineering, University of Baghdad, Iraq
abbas.abbas2001m@coeng.uobaghdad.edu.iq (corresponding author)

Shatha D. Mohammed
Civil Engineering Department, College of Engineering, University of Baghdad, Iraq
shatha.dh@coeng.uobaghdad.edu.iq

Received: 11 August 2023 | Revised: 27 August 2023 | Accepted: 30 August 2023

 DOI: https://doi.org/10.48084/etasr.6272

ABSTRACT

A Laced Reinforced Concrete (LRC) structural element comprises continuously inclined shear reinforcement in the form of lacing that connects the longitudinal reinforcements on both faces of the structural element. This study conducted a theoretical investigation of LRC deep beams to predict their behavior after exposure to fire and high temperatures. Four simply supported reinforced concrete beams of 1500 mm, 200 mm, and 240 mm length, width, and depth, respectively, were considered. The specimens were identical in terms of compressive strength ($f'_c \approx 40$ MPa) and steel reinforcement details. The same laced steel reinforcement ratio of 0.0035 was used. Three specimens were burned at variable durations and steady-state temperatures (one hour at 500 °C and 600 °C, and two hours at 500 °C). The flexural behavior of the simply supported deep beams, subjected to the two concentric loads in the middle third of the beam, was investigated with ABAQUS software. The results showed that the laced reinforcement with an inclination of 45° improved the structural behavior of the deep beams, and the lacing resisted failure and extended the life of the model. The optimal structural response was observed for the specimens. The laced reinforcement improved the failure mode and converted it from shear to flexure-shear failure. The parametric study showed that the lacing bars remarkably improved the strength of the deep beams and they were not affected more by the steady-state temperature and duration. Furthermore, a greater increase in load-carrying capacity was associated with an increase in the flexural diameter of approximately 12 and 16 mm by approximately 24.77% and 87.61%, respectively, compared to the reference LRC deep beams.

Keywords-laced reinforcement concrete; finite element method; self-compacting concrete; fire; high temperature; deep beam

I. INTRODUCTION

A Laced Reinforced Concrete (LRC) structure is a structural element that includes lacings and equal reinforcement on both the tension and compression faces. Due to the impact of the lacing reinforcement's truss action, the major flexural reinforcement bars are bound together on the element's face and the concrete components [1-2]. For concrete members, laced reinforcement increases ductility and improves confinement [3-5], providing greater shear resistance than traditional shear reinforcement (stirrups), which is significantly required in fortified structures [6]. In [7], it was shown that replacing the stirrups with lacings inclined at angles greater than 30° can convert the failure mode to pure flexural. In [8], the residual flexural strength of a slab was shown to be 81.5, 75, and 62.3% for fire temperatures of 300, 500, and 700 °C, respectively. Increasing compressive strength was found to decrease the percentage of remaining flexural strength, and rapid cooling had a greater impact on the residual flexural strength than slow cooling [9]. In [10], a specimen with a 0.0065 laced steel ratio increased its ultimate load by approximately 57% compared to one without a laced ratio. In [11], a laced reinforcement slab was compared with one without laced reinforcement, showing increase in cracking load and ultimate load of approximately 28, 45, 16, and 40%, respectively. Lacing bars were proposed as a low-cost alternative to traditional stirrups to improve the overall structural response of Self-Compacting Concrete (SCC) beams [12]. Deep beams are two-dimensional elements with a high depth to length ratio. The cross-sections exhibit nonlinear deformations under bending, resulting in a nonlinear distribution of the strains across them. Exposure to elevated temperatures, mainly caused by accidental fires, represents one

of the most severe exposure conditions for buildings and structures [13-14]. This study aimed to determine the efficiency of lacing reinforcement in post-fire deep beams and the contribution of the tension reinforcement to the performance of the lacing after exposure to fire.

II. DESCRIPTION OF THE TEST SPECIMENS

This study considered 4 simply supported specimens. All specimens were identical in terms of geometrical layout with a width of 200 mm, a depth of 240 mm, and an overall length of 1500 mm. The reinforcement details of 10 mm diameter for longitudinal tension reinforcement and laced reinforcement of 8 mm in diameter with an inclination of 45° as a shear reinforcement were according to ACI-318 and UFC 3-340-02 [15-16]. The test parameters were the steady-state temperature and the duration of the fire. Three specimens were tested under the effect of a static load (two-point load) after being exposed to a fire-flame effect of different steady-state temperatures (500 and 600°C) and duration of 1 and 2 hr, while the fourth was used as a reference specimen not affected by the fire-flame effect. Figure 1 shows the dimensions and details of the beam, and Table I shows the characteristics of the tested specimens.

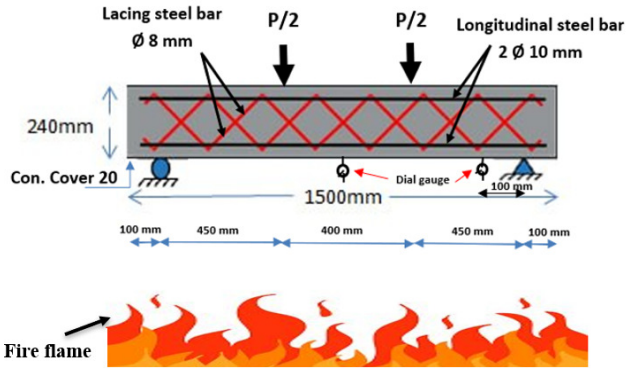

Fig. 1. Dimensions and details of the beam.

TABLE I. CHARACTERISTICS OF THE TESTED SPECIMENS

No.	Beam designation	Flexural diameter (mm)	Laced steel ratio	Steady-state temperature (°C)	Burning duration (h)
1	NF-REF	10	0.0035	No fire effect	-
2	F-500-1hr	10	0.0035	500	1
3	F-500-2hr	10	0.0035	500	2
4	F-600-1hr	10	0.0035	600	1

III. PROPERTIES OF THE HARDENED CONCRETE

The concrete mixtures were produced according to [17]. For the theoretical operation, hardened reinforced concrete in cubes and cylinders was tested using a specific concrete mix with specific proportions. The trial mix was cured at an average temperature of 28°C and a relative humidity of 60%. Table II shows the compressive strength (f_{cu}), splitting tensile strength (f_t), and modulus of elasticity (E_c) of the SCC to demonstrate the effect of exposure to fire on the mechanical properties of hardened concrete.

TABLE II. HARDENED PROPERTIES OF SCC

Steady-state temperature (°C)	Compressive strength (f_{cu}) (MPa)	Splitting tensile strength (f_t) (MPa)	Modulus of elasticity (E_c) (MPa)
25	57	4.01	31050
Duration (1hr)			
400	38	2.5	17100
500	35	2.33	16000
600	33	1.88	15000
700	20	1.33	12000
Duration (2 hr)			
500	32	1.91	13000
600	19	1.36	10000

IV. FINITE ELEMENT MODEL OF LRC DEEP BEAMS

To validate the experimental work, a 3D Finite Element Model (FEM) of the LRC deep beam specimen was carried out using ABAQUS to predict the flexural behavior. SCC was simulated in FEM using the Concrete Damage Plasticity Model (CDPM). All the material behaviors needed for the simulation were introduced directly into the selected models using the stress-strain behavior from the experimental investigation. A 3D 8-nodded linear brick element (C3D8R: 8-node linear hexahedral reduced integration hourglass control) was used to model the concrete beam and the supporting plate, while a 2-nodded element (T3D2: 2-nodded linear 3D truss element type) was used for the lacing steel bar, longitudinal steel bar, and stirrups. Figure 2 shows the discretized beam elements and the assembly of concrete and steel bars. Embedded region limitations were used to combine two surfaces during a simulation for the burned and reference beams, where every node on the surface was compelled to have the same motion as the closest point on the master surface with a frictionless contact property. Figure 3 shows the formulation of connecting interaction states in the model.

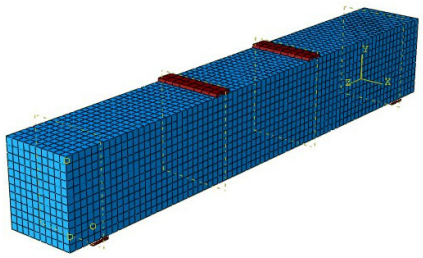

Fig. 2. Finite element model of the RC Beam in ABAQUS.

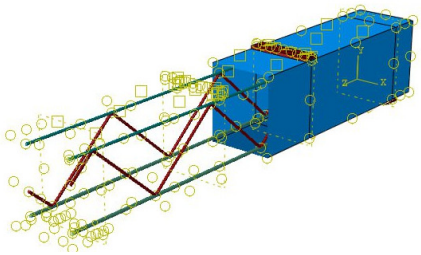

Fig. 3. Formulation of connected interaction-states in the model.

CDPM was used to simulate the nonlinear behavior of SCC [18-19]. This model requires the values of the modulus of elasticity and Poisson's ratio, and the description of compressive and tensile stress-plastic strain behavior, which were investigated experimentally and are shown in Table II. Table III shows the plastic damage parameters needed for the CDPM simulation in ABAQUS. The compressive stress-strain response of the SCC is necessary to analyze and design SCC members [20].

A. Concrete's Thermal Characteristics

Thermal conductivity defines a material's capacity to conduct heat by the ratio of heat flux and temperature gradient. It depicts the uniform flow of heat through the concrete of a thickness unit over a unit area subjected to a unit temperature difference between the two opposing faces. The conductivity of concrete is defined as a function of temperature [21]:

$$\lambda_c\left(\frac{\mathrm{W}}{\mathrm{mK}}\right) = 2 - \frac{0.24T}{120} + 0.012\left(\frac{T}{120}\right)^2,\ 20 \le T \le 1200^{\circ}\mathrm{C} \quad (1)$$

where λ_c is the thermal conductivity and T is the temperature.

Specific heat refers to the quantity of heat per mass unit required to elevate a substance's temperature by one degree. Specific heat is a function of temperature given by [21]:

$$C_c\left(\frac{\mathrm{J}}{\mathrm{kgK}}\right) = 900 + \frac{80T}{120} - 4\left(\frac{T}{120}\right)^2,\ 20 \le T \le 1200^{\circ}\mathrm{C} \quad (2)$$

where C_C is the specific heat and T is the temperature.

When exposed to a temperature change, concrete's isotropic nature causes it to exhibit thermal expansion. Stresses that result from non-uniform thermal expansion in concrete structures cause cracking. Eurocode 2 defines the thermal expansion of concrete as:

$$e_{th}(T) = \begin{cases} -1.8\times10^{-4} + 9\times10^{-6}T + 2.3\times10^{-11}T^3, & 20^{\circ}\mathrm{C} \le T \le 700^{\circ}\mathrm{C} \\ 14\times10^{-3}, & 700^{\circ}\mathrm{C} \le T \le 1200^{\circ}\mathrm{C} \end{cases} \quad (3)$$

where ε_{th} is the thermal expansion and T is the temperature.

TABLE III. CONCRETE DAMAGE PLASTICITY PARAMETERS

Parameter	Selected value
Material model	CDP model
Dilation angle	45
€	0.1
Fb_0/fc_0	1.16
K	0.667
Viscosity parameter	0.0001

B. Steel's Thermal Properties

Steel has a variety of mechanical characteristics, including mass density, Young's modulus, and Poisson's ratio. Steel maintains its mass density (7850 kg/m^3) even at high temperatures. Temperature impacts steel's Young modulus. The values for the steel modulus of elasticity (E_s) at high temperatures are prescribed by Eurocode 3 [22]. On the other hand, Poisson's ratio is considered to be constant (0.3) at all temperatures [23]. The uniaxial stress-strain relationship for steel in the FEMs was idealized as a bilinear curve and was expected to behave as an elastic-plastic model with strain hardening. Thermal conductivity (λ_c), specific heat (C_s), and thermal expansion (ε_{th}) are all thermal properties of steel. The following formulae are used by Eurocode 3 to define these attributes as functions of temperature:

$$\lambda_c\left(\frac{\mathrm{W}}{\mathrm{mK}}\right) = \begin{cases} 54 - 3.33\times10^{-2}T, & 20 \le T < 800^{\circ}\mathrm{C} \\ 27.3, & 800 < T < 1200^{\circ}C \end{cases} \quad (4)$$

$$C_s(\mathrm{J/kgK}) = \begin{cases} 425 + 7.73\times10^{-1}\mathrm{T} - 1.69\times10^{-3}\mathrm{T}^2 + 7.73\times10^{-6}\mathrm{T}^3, \\ \qquad 20 \le \mathrm{T} < 600^{\circ}\mathrm{C} \\ 666 + \frac{13003}{738-\mathrm{T}},\ 600 < \mathrm{T} \le 735^{\circ}\mathrm{C} \\ 545 + \frac{17820}{T-731},\ 735 < \mathrm{T} \le 900^{\circ}\mathrm{C} \\ 650,\ 900 < \mathrm{T} \le 1200^{\circ}\mathrm{C} \end{cases} \quad (5)$$

$$\varepsilon_{\mathrm{th}}(\mathrm{T}) = \begin{cases} -2.416\times10^{-4} + 1.5\times10^{-5}T + 0.4\times10^{-8}T^2, \\ \qquad 20 \le T < 750^{\circ}\mathrm{C} \\ 1.1\times10^{-2},\ 750 < T \le 860^{\circ}\mathrm{C} \\ -6.2\times10^{-4}2\times10^{-5}T,\ 860 < T \le 1200^{\circ}\mathrm{C} \end{cases} \quad (6)$$

V. RESULTS AND DISCUSSION

A. FEA Observations

The crack patterns observed in the FEMs showed a combined flexure-shear failure, as the lacing reinforcement improves the behavior of the specimens and converts the failure mode from shear to flexure-shear failure. The first flexural crack was observed on the tension surface directly below the loading points, where the bending moment was the largest. Thereafter, inclined cracks appeared in the shear span when increasing the applied load. As the load increased, both crack types grew, enlarged, and propagated upward, causing the failure of these beams, followed by the crushing of the concrete. For an even comparison of responses of different specimens in finite element analysis, all FEMs were compared at the ultimate load. The damage region for tension and compression is described by concrete compression damage (dc) and concrete tension damage (*dt*), according to the ABAQUS software documentation. Figure 4 shows the finite element analysis observations for crack patterns.

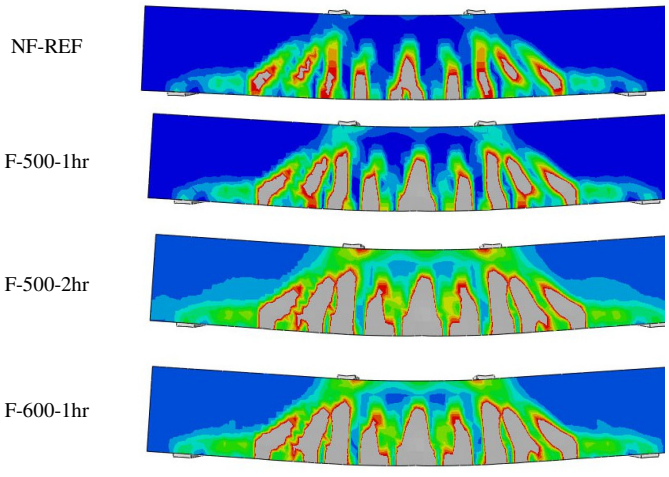

Fig. 4. Tension cracks pattern for specimens.

B. Load-Displacement Behavior

In terms of the effect of the burning duration, Figure 5 shows the load-displacement curves for the burning specimens,

indicating a decrease in load-carrying capacity with increasing fire duration compared to the reference beam. The decrease was approximately 18.58 and 26.55% with increasing fire duration from 1 to 2 hr at 500 °C, respectively. Figure 5 also shows that an increase in steady-state temperature resulted in a decrease in load-carrying capacity compared to the reference beam. The decrease was approximately 18.58 and 30.08% with increasing steady-state temperature from 500 to 600 °C, respectively, at 1 hr of burn duration.

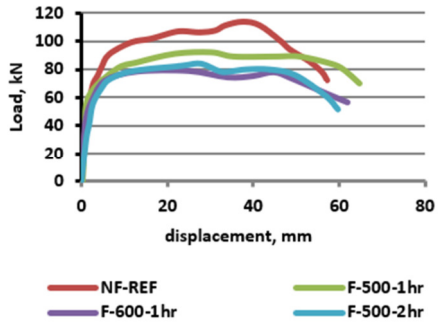

Fig. 5. Load-displacement behavior.

The vertical deflection at mid-span was measured for the ultimate load for all specimens. Compared to the reference specimen, a decrease in deflection was observed at the ultimate load, of approximately 19.87, 25.69, and 33.85%, with increasing steady-state temperature and duration. Table IV shows the variation of the ultimate load and deflection. The effect of lacing reinforcement was clear, when the beam failed, it got up again and showed resistance, improving the specimen's strength and leading to an increase in load-carrying capacity and displacement.

TABLE IV. ULTIMATE LOAD AND DEFLECTION.

Specimens	P_u (kN)	Variation %	Δu (mm)	Variation %
NF-REF	113	-	37.64	-
F-500-1hr	92	-18.58	30.16	-19.87
F-500-2hr	83	-26.55	27.97	-25.69
F-600-1hr	79	-30.08	24.90	-33.85

In terms of the energy absorbed by the LRC deep beams exposed to fire, the burning reduced the toughness of the specimens. The absorbed energy at the ultimate load was 3685.44, 2425.68, 1805.70, and 1572.85 kNmm for the specimens NF-REF, F-500-1hr, F-500-2hr, and F-600-1hr, respectively, as shown in Figure 6.

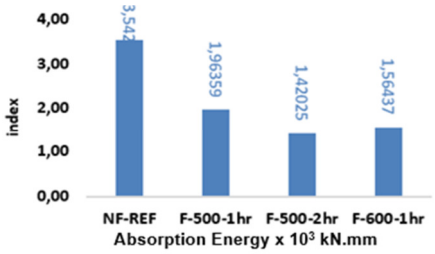

Fig. 6. Absorption energy index for laced reinforcement specimens.

VI. PARAMETRIC STUDY

Two diameters of flexural bars, 12 and 16 mm, were selected to investigate the effect of the area of the flexural bars on the structural behavior of the concrete deep beams. The other properties were kept constant and the adopted lacing angle was 45°. Figure 7 shows the load-deflection responses of the two beams, indicating a larger increase in load-carrying capacity with an increase in the flexural diameter from 10 to 12 and 16 mm, by approximately 24.77 and 87.61%, respectively. The tension and lacing strain values at the flexural span achieved a 0.003 micro-strain, which is presented in Figure 8.

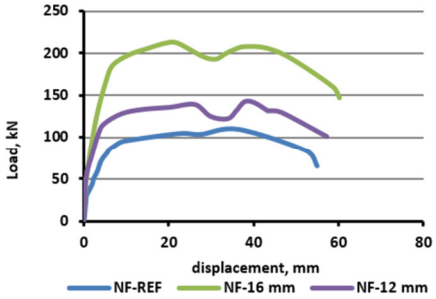

Fig. 7. Influence of the flexural bar diameter.

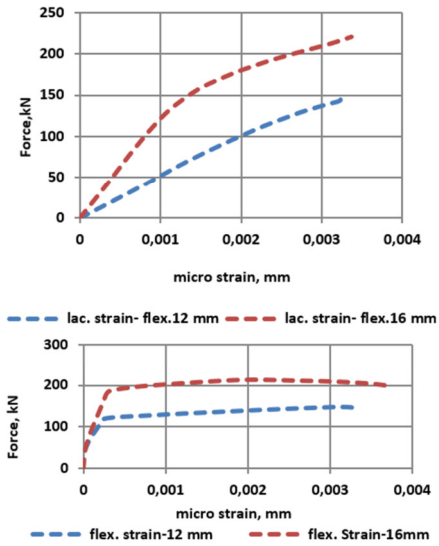

Fig. 8. Load-steel strains with different diameters of flexural rebar.

To investigate the influence of various steady-state temperatures and durations on the behavior of LRC deep beams for SCC, burning of 400 and 700 °C for 1jr and 600 °C for 2 hr were numerically investigated while keeping the other properties constant. The results confirmed that the laced bars remarkably improved the strength of the deep beams and were not affected more by the steady-state temperature and duration. A decrease in the load-carrying capacity was observed with increasing steady-state temperature and duration compared to the reference beam. On the other hand, Figure 9 shows the displacement at the failure load with increasing steady-state temperature and duration of the fire. Figure 10 shows the strains in lacings and tension flexural reinforcement located at

the shear span of the beams with different steady-state temperatures at various durations.

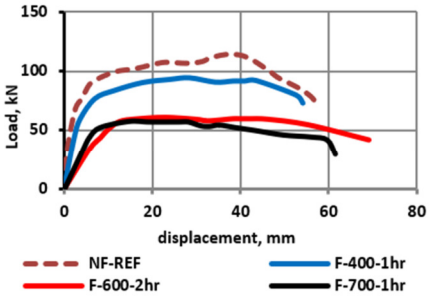

Fig. 9. Load displacement behavior for changing steady-state temperature.

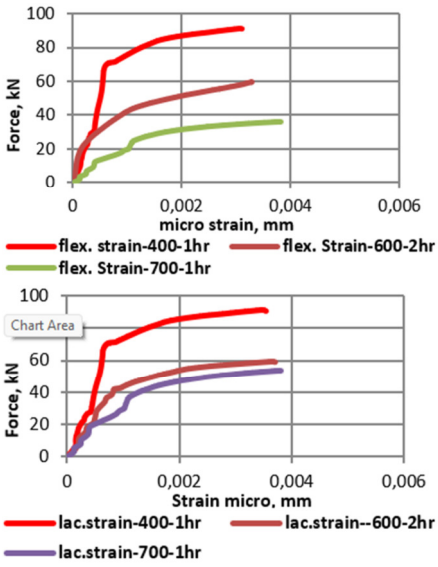

Fig. 10. Load-steel strains with changing temperature.

VII. CONCLUSIONS

In this study, laced reinforcement with an inclination of 45° in deep beams after exposure to fire flame was numerically investigated. The following conclusions were derived:

- Laced reinforcement improved the structural behavior of the deep beams. The behavior of beams was found to be significantly affected by the lacing. The lacing resists failure and extends model life. Optimal structural response was observed for burned specimens compared to the reference beam.
- The laced reinforcement converts the failure mode of a deep beam from shear to combined flexure-shear failure.
- The laced reinforcement increased flexural toughness at the failure load for the burned specimens by increasing the resistance of the beam, which improved the load-displacement behavior.
- The finite element analysis observations of the parametric study showed that the lacing bars remarkably improved the strength of the deep beams and were not affected more by the steady-state temperature and duration when they were increased to 700 °C and 2 hr, respectively.

REFERENCES

[1] N. Sudharsan, C. J. B. Grant, P. Murthi, K. Poongodi, and P. M. Kumar, "A Comparative Experimental Investigation on Laced Reinforced Concrete Beam and Conventional Beam under Monotonic Loading," *IOP Conference Series: Earth and Environmental Science*, vol. 822, no. 1, Apr. 2021, Art. no. 012034, https://doi.org/10.1088/1755-1315/822/1/012034.

[2] S. Narayanasamy and B. Grant, "Structural Behaviour of Laced Reinforced Concrete Elements - A survey," *International Journal of Current Engineering and Scientific Research*, vol. 4, no. 12, pp. 36–41, Jan. 2017.

[3] N. Anandavalli, N. Lakshmanan, A. Prakash, J. Rajasankar, and N. R. Iyer, "Numerical Investigations on a Blast Loaded Laced Reinforced Concrete Structure using an Equivalent Constitutive Property," *Journal of The Institution of Engineers (India): Series A*, vol. 96, no. 4, pp. 311–318, Dec. 2015, https://doi.org/10.1007/s40030-015-0139-6.

[4] A. I. Abdullah and S. D. M. Al-Khazraji, "Structural Behavior of High Strength Laced Reinforced Concrete One Way Slab Exposed to Fire Flame," *Civil Engineering Journal*, vol. 5, no. 12, pp. 2747–2761, Dec. 2019, https://doi.org/10.28991/cej-2019-03091446.

[5] N. Anandavalli *et al.*, "Behaviour of a Blast Loaded Laced Reinforced Concrete Structure," *Defence Science Journal*, vol. 62, no. 5, pp. 284–289, Sep. 2012, https://doi.org/10.14429/dsj.62.820.

[6] G. M. Colyvas, Y. Malecot, Y. Sieffert, S. Aboudha, and C. Kanali, "Behavior of Reinforced Concrete Beams using Wire Rope as Internal Shear Reinforcement," *Engineering, Technology & Applied Science Research*, vol. 10, no. 4, pp. 5940–5946, Aug. 2020, https://doi.org/10.48084/etasr.3496.

[7] T. S. Al-Gasham, J. M. Mhalhal, and S. R. Abid, "Flexural Behavior of Laced Reinforced Concrete Moderately Deep Beams," *Case Studies in Construction Materials*, vol. 13, Dec. 2020, Art. no. e00363, https://doi.org/10.1016/j.cscm.2020.e00363.

[8] A. A. Hammadi, A. F. Izzat, and J. A. Farhan, "Effect of Fire Flame (High Temperature) on the Self Compacted Concrete (SCC) One Way Slabs," *Journal of Engineering*, vol. 18, no. 10, pp. 1083–1099, Jul. 2023, https://doi.org/10.31026/j.eng.2012.10.01.

[9] S. D. Mohammed and N. M. Fawzi, "Fire Flame Influence on the Behavior of reinforced Concrete Beams Affected by Repeated Load," *Journal of Engineering*, vol. 22, no. 9, pp. 206–223, Sep. 2017, https://doi.org/10.31026/j.eng.2016.09.13.

[10] H. A. Jabir, "The behavior of one-way concrete slab with lacing reinforcement subjected to static and repeated load," Ph.D. dissertation, University of Baghdad, Iraq, 2016.

[11] A. F. Hallawi and A. H. A. Al-Ahmed, "Enhancing the Behavior of One-Way Reinforced Concrete Slabs by Using Laced Reinforcement," *Civil Engineering Journal*, vol. 5, no. 3, pp. 718–728, Mar. 2019, https://doi.org/10.28991/cej-2019-03091282.

[12] T. Ofuyatan, F. A. Olutoge, and A. Olowofoyeku, "Durability Properties of Palm Oil Fuel Ash Self Compacting Concrete," *Engineering, Technology & Applied Science Research*, vol. 5, no. 1, pp. 753–756, Feb. 2015, https://doi.org/10.48084/etasr.524.

[13] N. F. Hussen and S. D. Mohammed, "Influence of Fire-Flame Duration and Temperature on the Behavior of Reinforced Concrete Beam Containing Water Absorption Polymer Sphere; Numerical Investigation," *Journal of Engineering*, vol. 28, no. 11, pp. 67–84, Nov. 2022, https://doi.org/10.31026/j.eng.2022.11.06.

[14] M. Baghdadi, M. S. Dimia, and D. Baghdadi, "A Parametric Study of Fire-Damaged Reinforced Concrete Columns under Lateral Loads," *Engineering, Technology & Applied Science Research*, vol. 12, no. 5, pp. 9113–9119, Oct. 2022, https://doi.org/10.48084/etasr.5172.

[15] J. P. Moehle, "Key Changes in the 2019 Edition of the ACI Building Code (ACI 318-19)," *Concrete International*, vol. 41, no. 8, pp. 21–27, Aug. 2019.

[16] "Guidelines for Self-Compacting Concrete," European Federation for Specialist Construction Chemicals and Concrete Systems, Norfolk, UK, 2002.

[17] "The European Guidelines for Self-Compacting Concrete," European Federation for Specialist Construction Chemicals and Concrete Systems, Norfolk, UK, 2005.

[18] M. Neuenschwander, M. Knobloch, and M. Fontana, "Suitability of the damage-plasticity modelling concept for concrete at elevated temperatures: Experimental validation with uniaxial cyclic compression tests," *Cement and Concrete Research*, vol. 79, pp. 57–75, Jan. 2016, https://doi.org/10.1016/j.cemconres.2015.07.013.

[19] L. T. Yaw, J. B. Osei, and M. Adom-Asamoah, "On The Non-Linear Finite Element Modelling of Self-Compacting Concrete Beams," *Journal of Structural Transportation Studies*, vol. 2, no. 2, 2017.

[20] J. Lubliner, J. Oliver, S. Oller, and E. Oñate, "A plastic-damage model for concrete," *International Journal of Solids and Structures*, vol. 25, no. 3, pp. 299–326, Jan. 1989, https://doi.org/10.1016/0020-7683(89)90050-4.

[21] "Eurocode 2: Design of concrete structures," European Committee for Standardization, Brussels, Belgium, European Standard EN 19992-1-2, 2004.

[22] A. Nussbaumer, L. Borges, and L. Davaine, Fatigue Design of Steel and Composite Structures: Eurocode 3: Design of Steel Structures, Part 1-9 Fatigue; Eurocode 4: Design of Composite Steel and Concrete Structures. Berlin, Germany: European Convention for Constructional Steelwork, 2011.

[23] S. J. George and Y. Tian, "Structural Performance of Reinforced Concrete Flat Plate Buildings Subjected to Fire," *International Journal of Concrete Structures and Materials*, vol. 6, no. 2, pp. 111–121, Jun. 2012, https://doi.org/10.1007/s40069-012-0011-2.